Supplement of Atmos. Chem. Phys., 26, 8783–8807, 2026
https://doi.org/10.5194/acp-26-8783-2026-supplement


Atmospheric Chemistry and Physics
Open Access
EGU

*Supplement of*

# Tropospheric ozone trends and drivers at a Southern Hemisphere background site in Chile

**Laura Gallardo et al.**

*Correspondence to:* Laura Gallardo (lgallard@u.uchile.cl)

**Supplementary Material**

## *Population and infrastructure around Tololo*

The population of the La Serena and Coquimbo conurbation has more than doubled between the census 1992 and 2024 (https://www.ine.gob.cl/), reaching today roughly 543 k inhabitants (https://www.bcn.cl). Smaller towns of more than 10 k inhabitants are situated nearby: Vicuña (20 km NE), and Andacollo (30 km SW). Vicuña grew 41% from 1992 to 2024 having today ca. 31 k inhabitants, and Andacollo decreased by 3% over the same period, having today ca. 12 k inhabitants. Finally, Ovalle (60 km SW) grew by 46% between 1992 and 2024, and today has a population of ca. 124 k inhabitants. Also, the number of motor vehicles has substantially grown between 1992 and present, reaching today ca. 298 k units in La Serena and Coquimbo. However, due to the implementation of standards and technological changes in Chile, vehicles emissions are estimated to be similar (NOx) or much lower (CO, VOC) between 1992 and 2020 (Osses et al., 2022). Figure S 1 shows population density as well as infrastructure in the surroundings of Tololo. Available air quality monitoring stations run by the Ministry of Environment at Coquimbo-La Serena and Andacollo only measure particles mass concentrations (https://sinca.mma.gob.cl/).

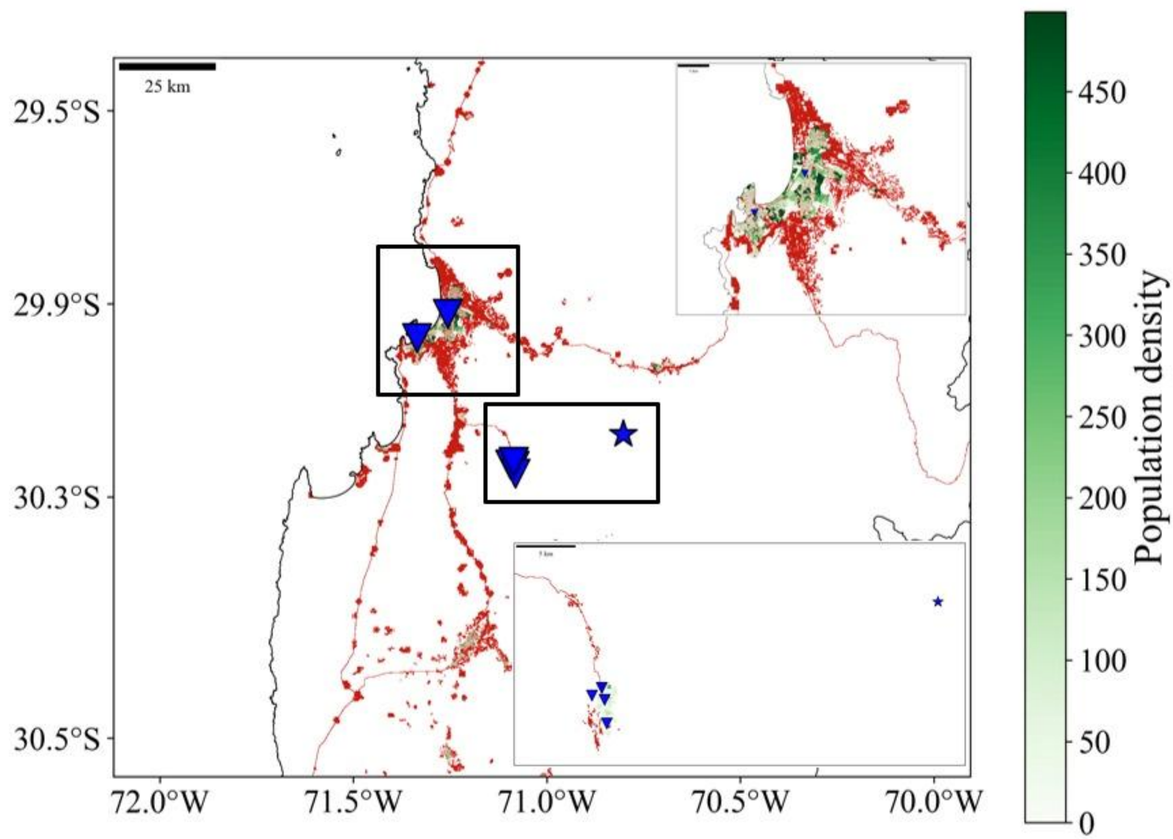


**Figure S 1. This figure shows population density (inhabitants per census block) in green and infrastructure (red) in the surroundings of Tololo, which is indicated by the star. Triangles indicate the location of air quality monitoring stations run by the**

Ministry of Environment (https://sinca.mma.gob.cl). Population density corresponds to the latest available census data of 2017 as described in https://ideocuc-ocuc.hub.arcgis.com/ (Accessed in January 2025). Infrastructure was downloaded from https://chile.mapbiomas.org/ (Accessed January 2025).

## *Bias correction of ERA 5 data*

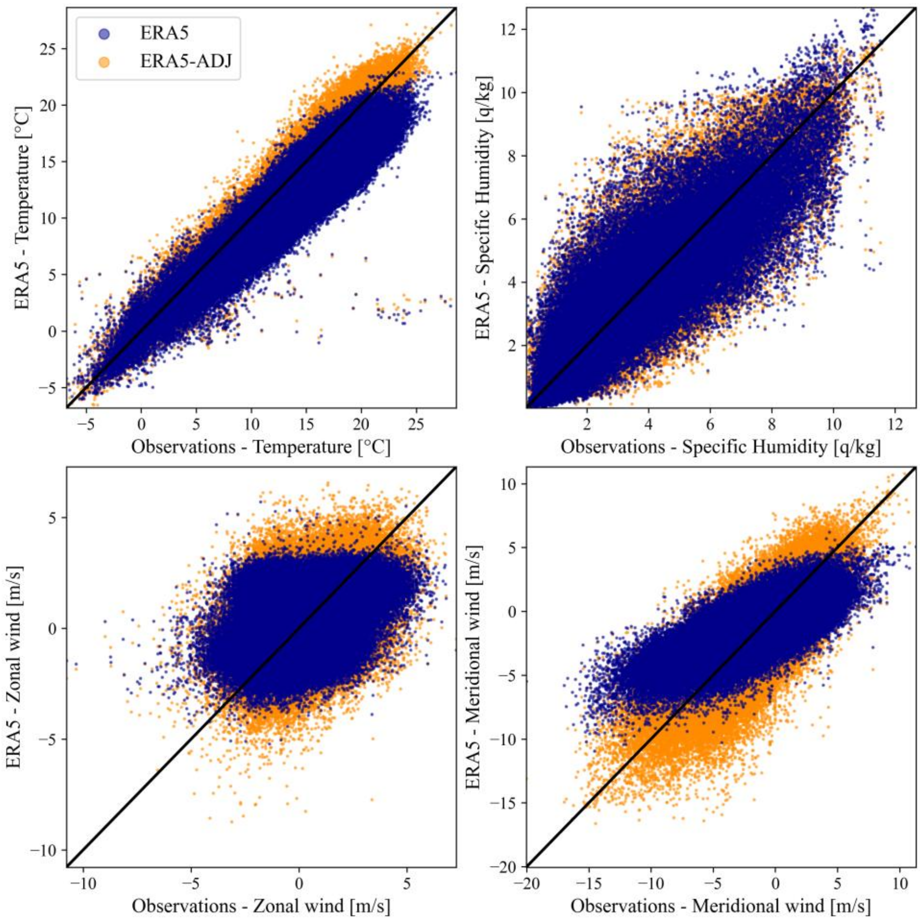


**Figure S 2. Scatterplots between observed meteorological time series, and corresponding time series obtained from ERA5 and adjusted ERA5 time series. Adjusted ERA5 time series were obtained according to the bias correction described in section 2.3. Meteorological variables shown are: temperature, specific humidity, zonal wind and meridional wind.**

### *Methane at Rapa Nui and Tololo*

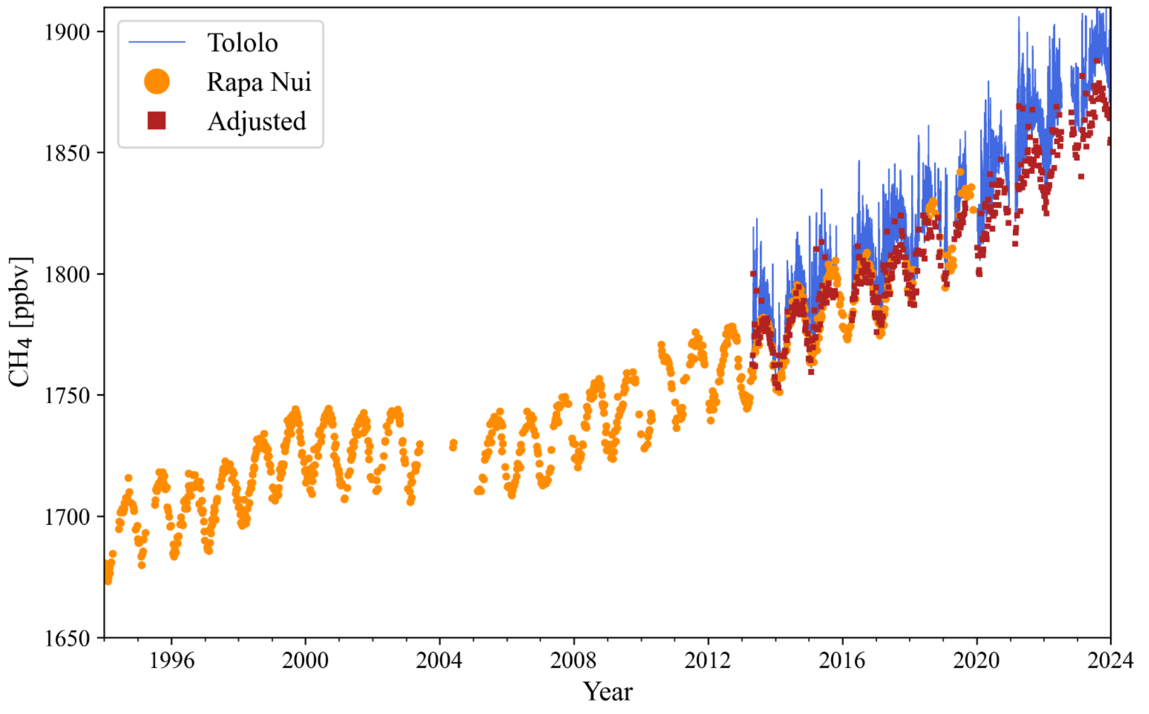


**Figure S 3. Time series of observed methane ($CH_4$) in Rapa Nui (orange), Tololo (blue) and adjusted methane in Rapa Nui (red). The adjusted methane time series was obtained according to a simple linear regression described in section 2.4.**

## *Bias correction of simulated CO*

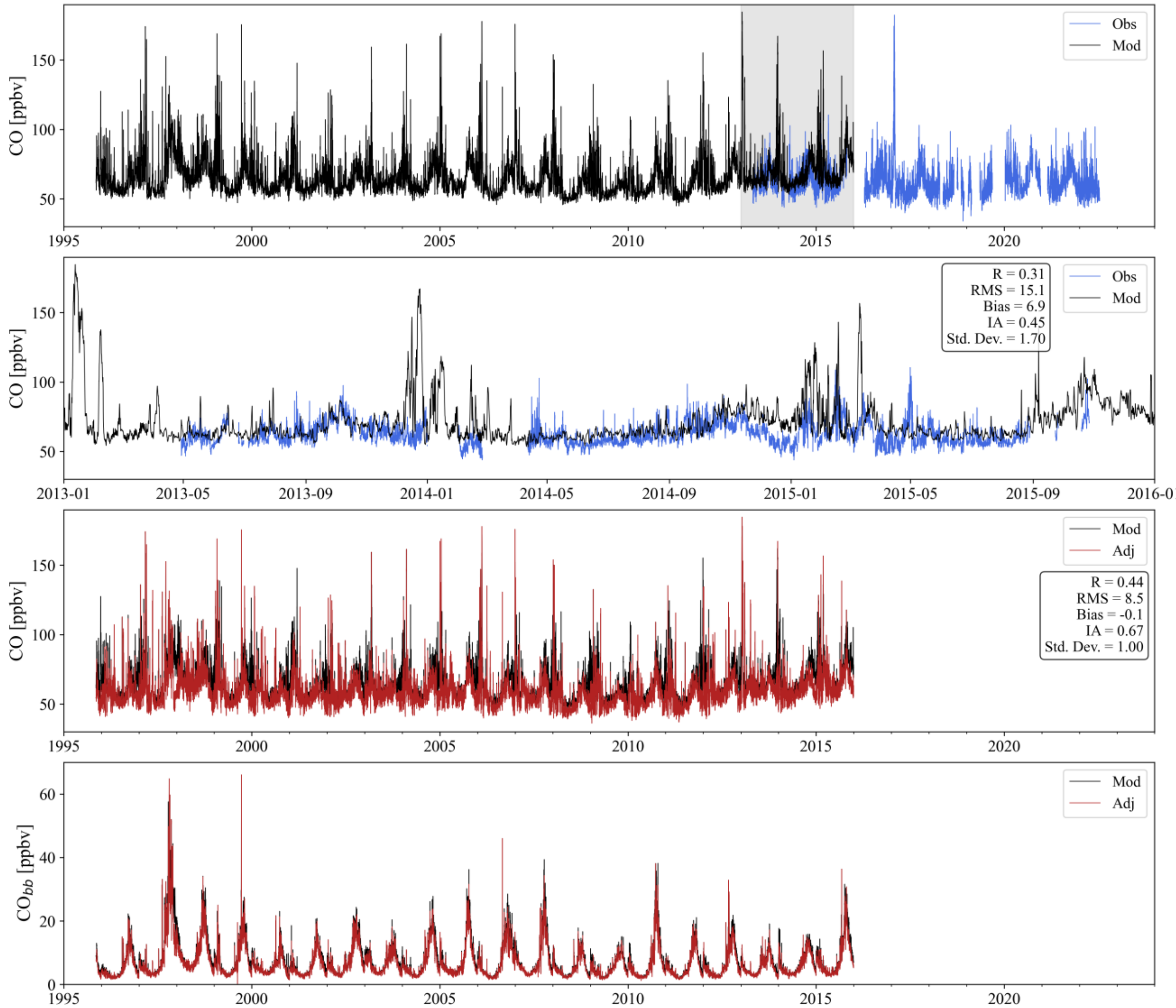


**Figure S 4. Upper panel shows observed (Obs, blue) and simulated (Mod, black) carbon monoxide (CO) mixing ratios (blue and black respectively). The grey shading indicates the overlap period between measurements and simulations. The second panel corresponds to a zoom over the overlap period before the bias correction. The third panel shows the simulated (Mod, black) and adjusted (Adj, bias corrected, red) time series. The lower most panel shos the simulated and adjusted curves for the estimated biomass burning (Cobb) signal. The middle panels also show error statistics (R: Pearson correlation; RMS: Root Mean Square Error; IA: Index of Agreement; Std. Dev: Normalized standard deviation as described in (Brasseur and Jacob, 2017)).**

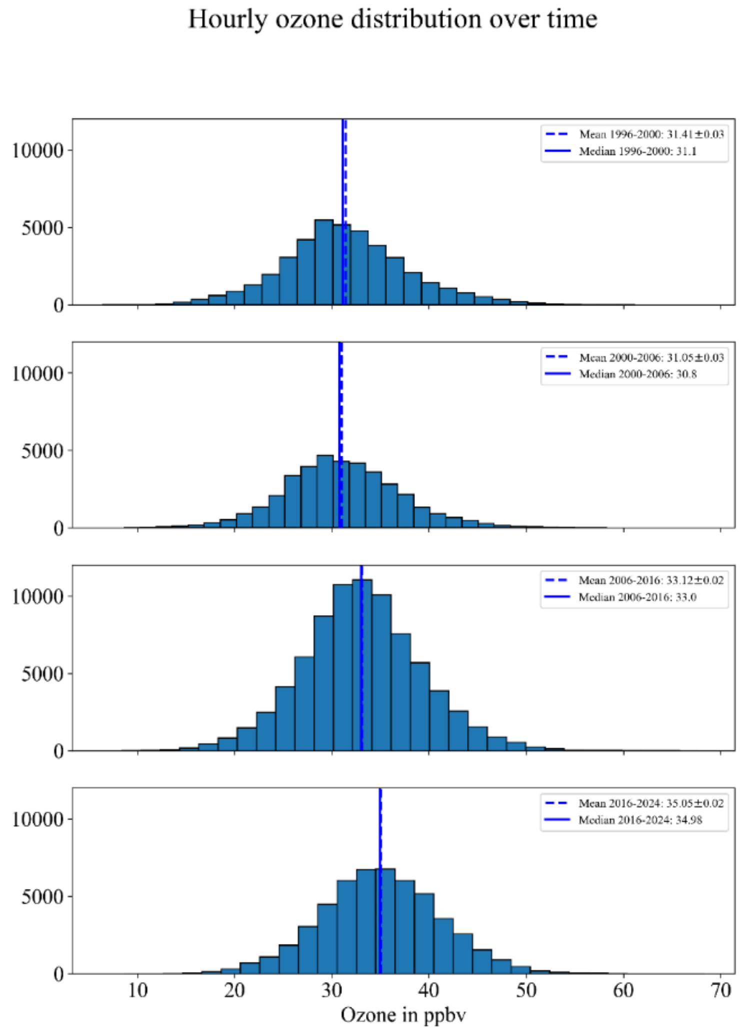


**Figure S 5. Ozone hourly distributions over four periods, chosen according to change points in the methane time series. Each panel shows in the vertical axis the frequency, and in the horizontal the ozone values. Also indicated are the distribution's mean (dashed line) and median (solid line). In the corresponding legends one can read the mean ± the standard error, and the median.**

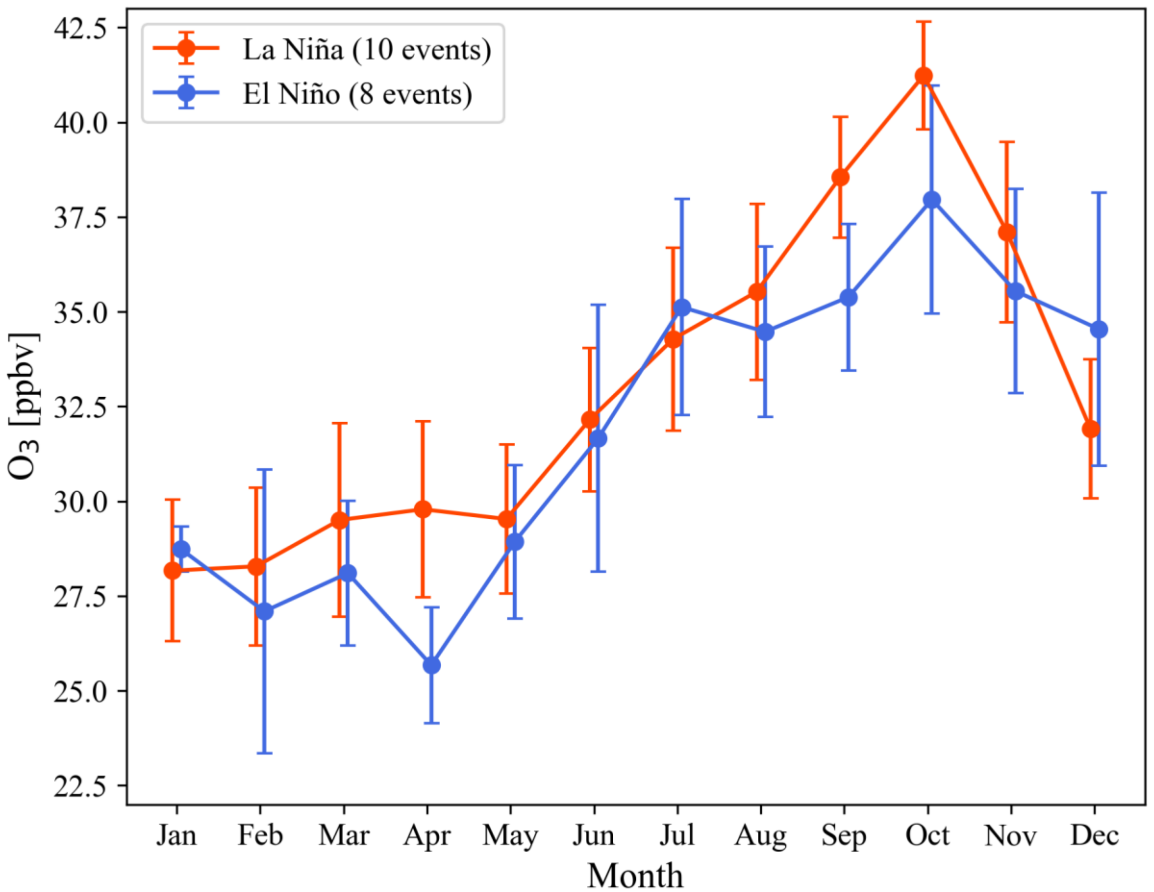


**Figure S 6. Annual cycle of ozone observations in Tololo during El Niño and La Niña conditions. El Niño (La Niña) conditions were defined as consecutive months (at least 3 months) when MEI index was greater (less) than 0.5 (-0.5). In parentheses is indicated the number of periods with El Niño/La Niña conditions between November 1995 and 2023.**

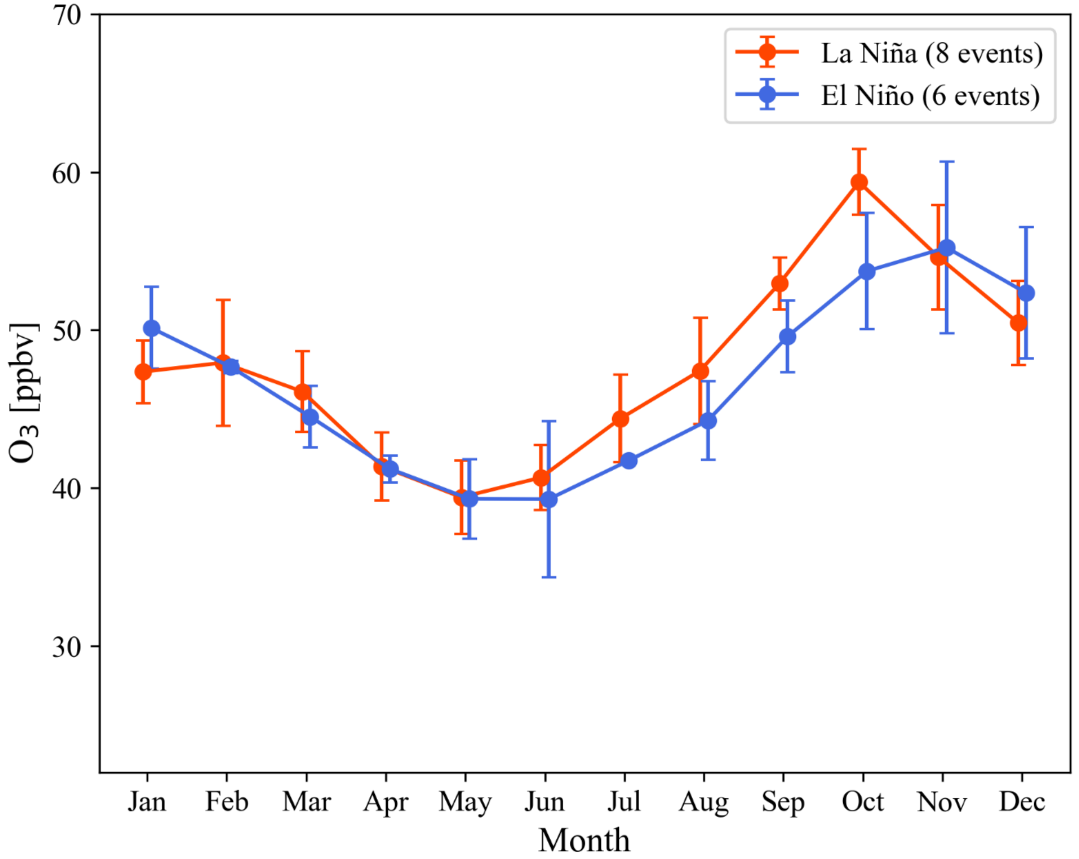


**Figure S 7. As in the previous figure but for model outputs.**

**Cluster analysis of air of stratospheric and upper troposphere origin**

Using k-means, we identified four groups of synoptic configurations for high ozone and low humidity events at Tololo. These groups, i.e, 1,2,3 and 4 contain 67, 89, 51 and 45 members respectively.

The first cluster shows a quadrupole over Southern South America, with a subtropical high over the western coast and a subtropical low over the continent. Opposite lows and highs occur over the extratropical regions. Day zero marks the arrival of the leading edge of the subtropical high over the region, with strong subsidence over the region of interest in Northern Chile.

The second cluster resembles a more zonal wave train travelling towards the subtropics from the extratropics, during day 0 and similarly to the previous cluster, the more significant feature is the leading edge of the anticyclonic anomaly associated with a stronger feature of subsidence around 30ºS (Fig. S10).

Cluster 3 shows a larger pattern featuring an approximately wavenumber 4 perturbation, with strong subsidence between the rear edge of continental low and the leading edge of the anticyclonic anomaly over the western coast of South America (Fig. S12). Interestingly, perturbations of similar wavelength and progression can be excited as a result of MJO tropical forcing (Matus et al, 2025)

Finally, cluster 4 also depicts a quadrupole structure over Southern South America, only this time of the opposite sign as the cluster 1 quadrupole (Fig. S14). Notice that a subtropical low is located well off the coast of South America, centered at about 100ºW and 25ºS which resembles the composite of D cases found in Rondanelli et al (2002) for increases of ozone at Cerro Tololo.

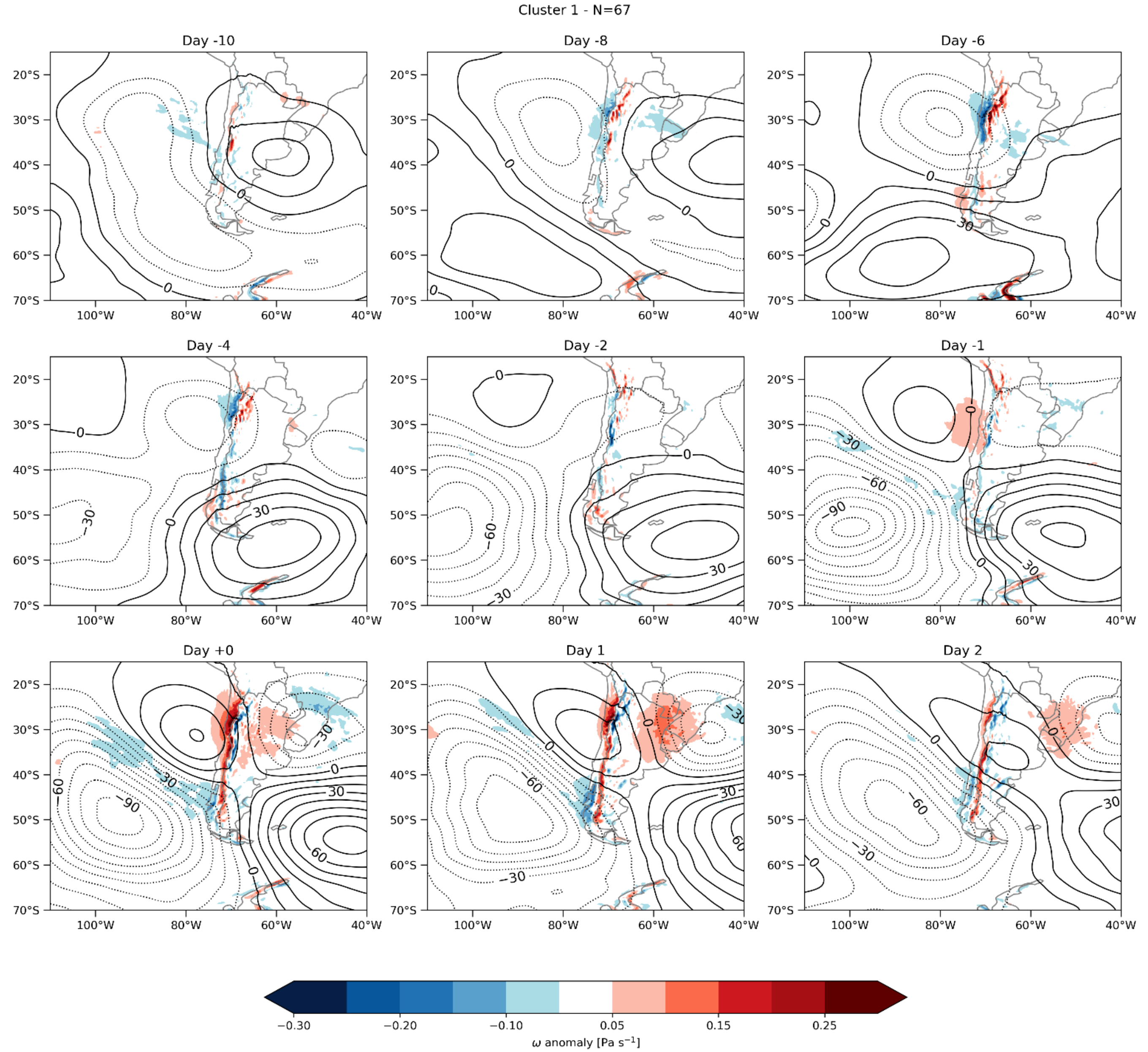


**Figure S 8. Composite maps of geopotential height and vertical velocity anomalies at 500 hPa during SUTO events for cluster 1. Contours denote geopotential height anomalies in meters, where positive (negative) anomalies are solid (dotted) contours. Shaded areas denote vertical velocity anomalies in Pa/s.**

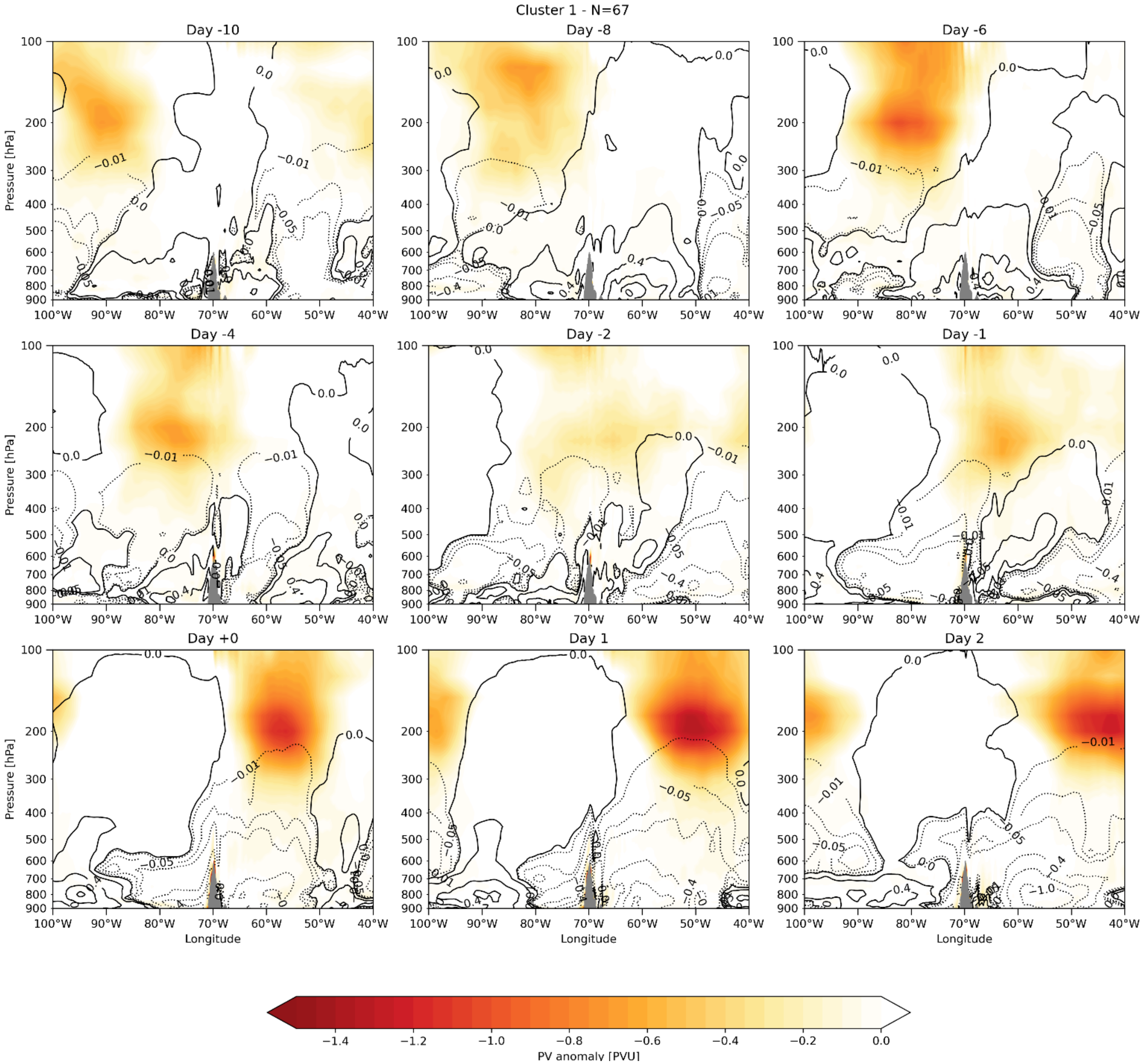


**Figure S 9. Composite of longitude-pressure cross-section of potential vorticity and specific humidity anomalies between 900 and 200 hPa during SUTO events for cluster 1. Contours denote specific humidity anomalies in g/kg, where positive (negative) anomalies are solid (dotted) contours. The shaded area denotes potential vorticity anomalies in potential vorticity units (PVU).**

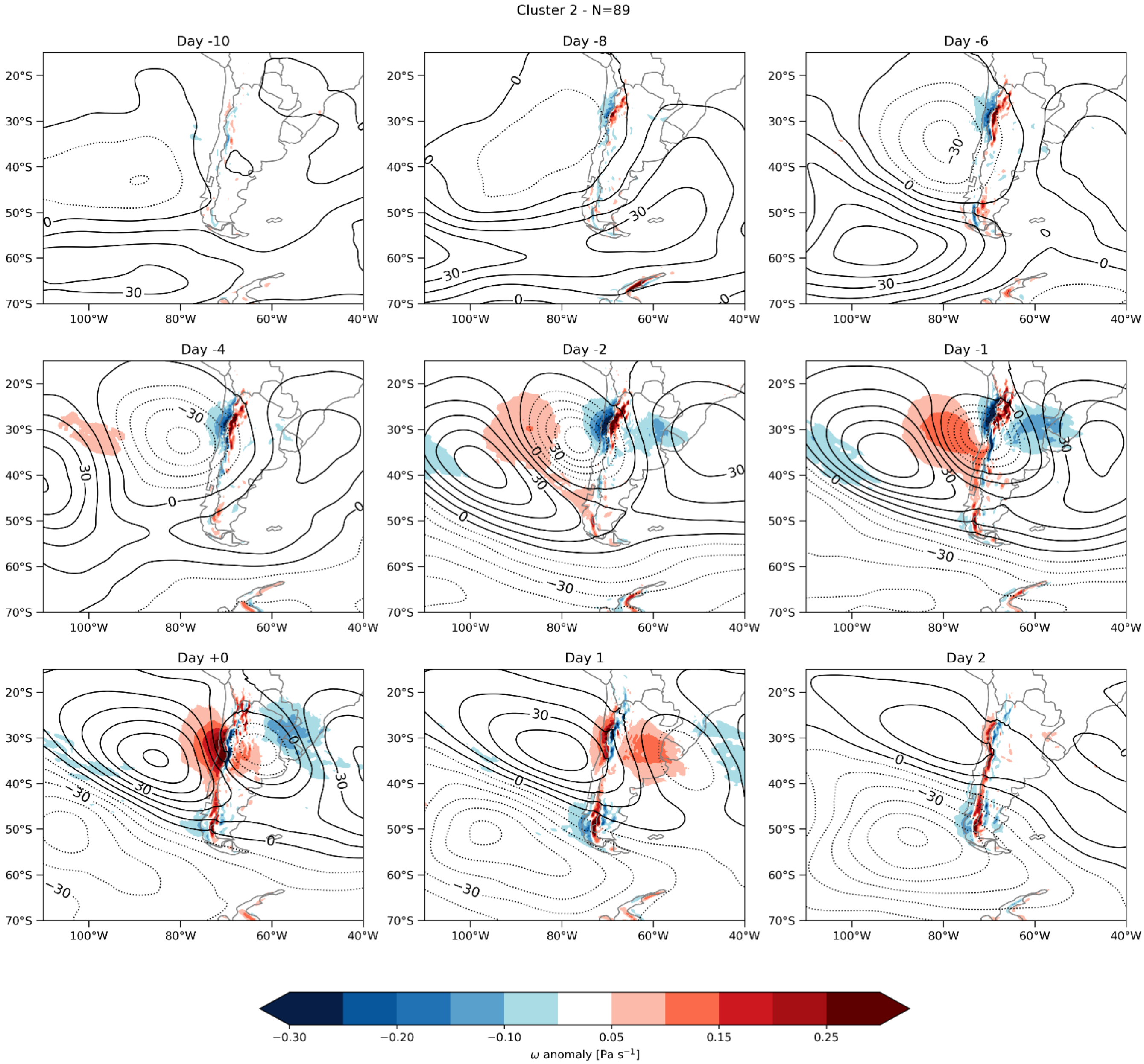


**Figure S 10. Like Figure S 8 but for cluster 2.**

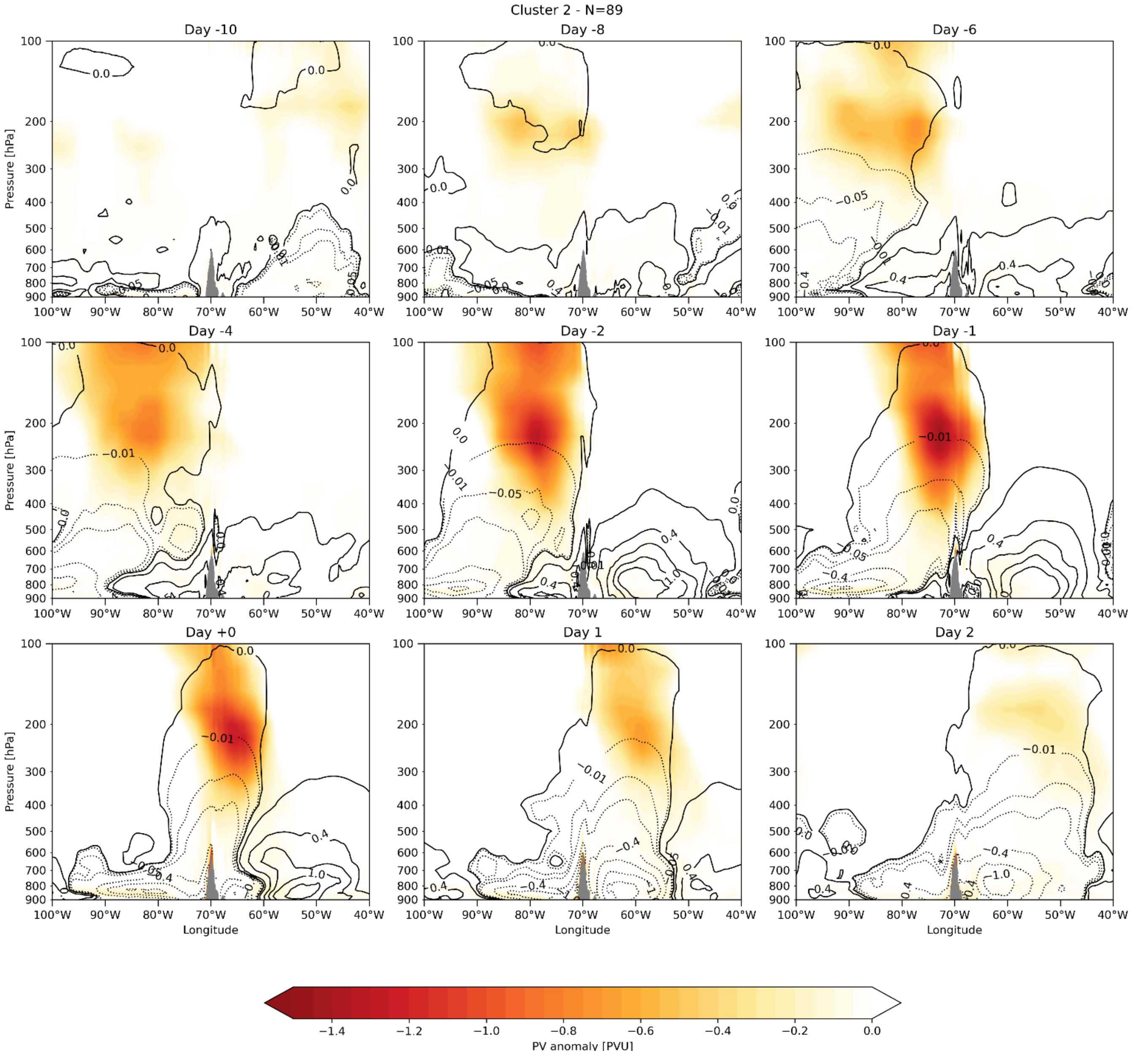


**Figure S 11. Like Figure S 9 but for cluster 2.**

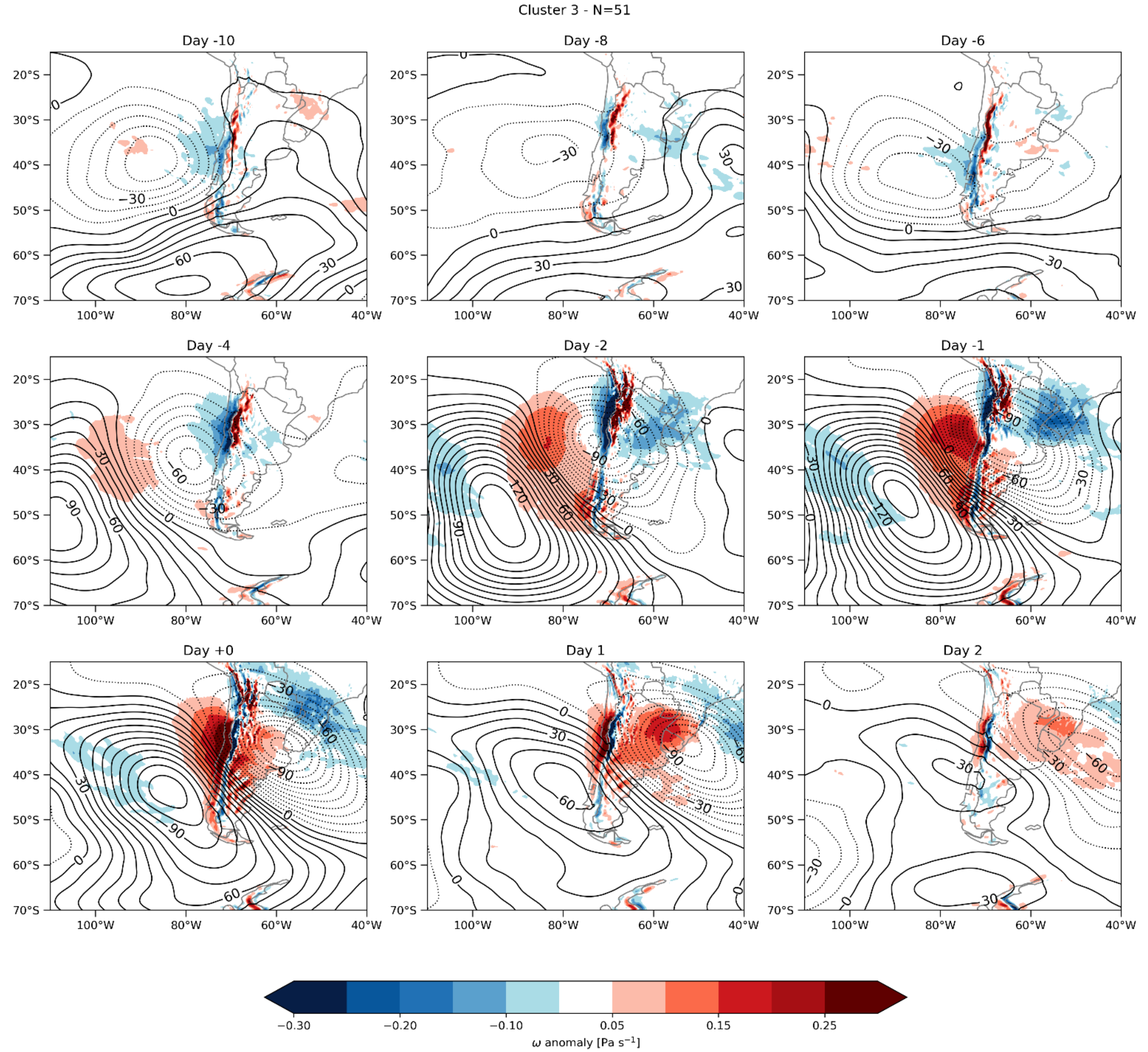


**Figure S 12. Like Figure S 8 but for cluster 3.**

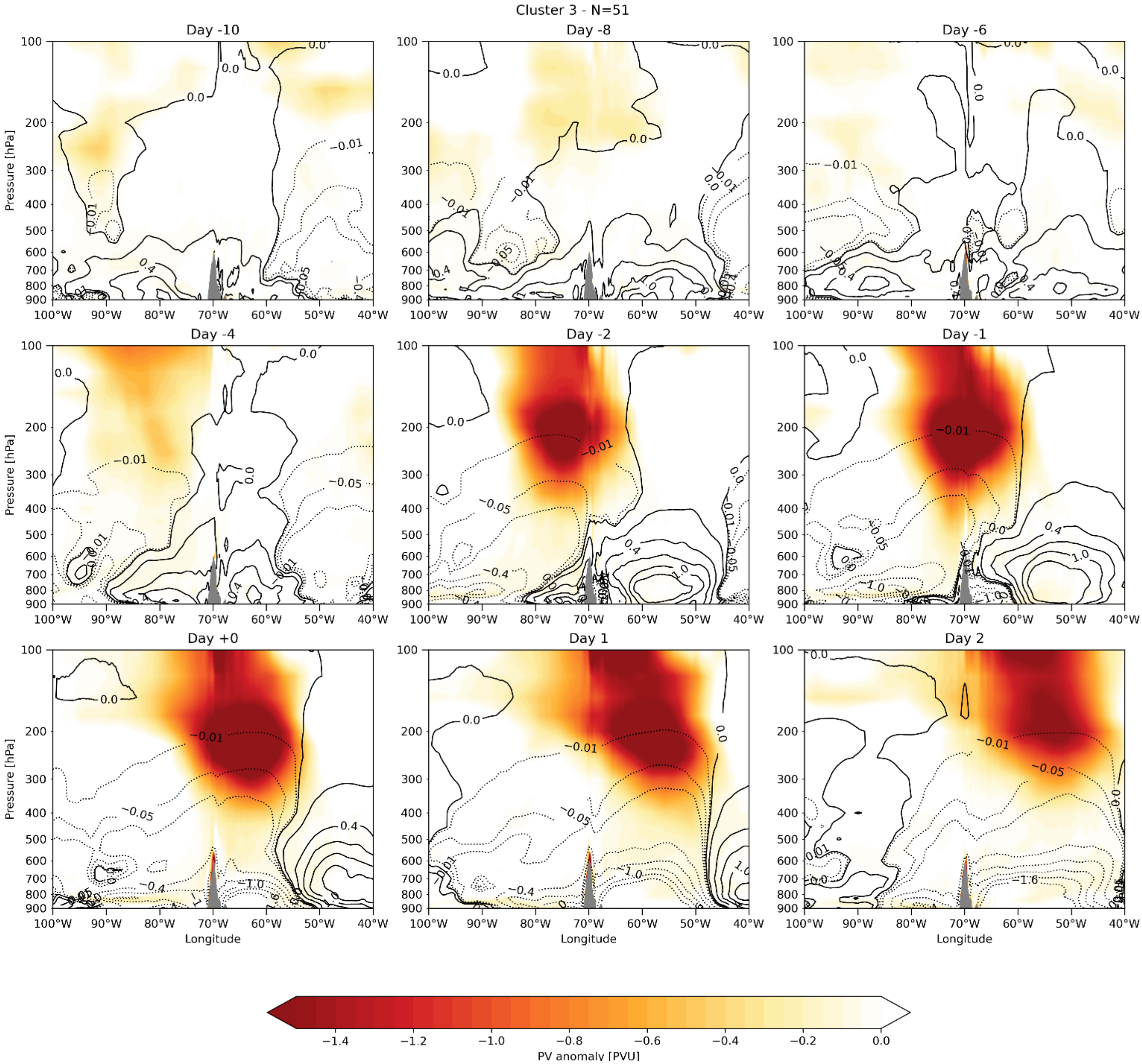


**Figure S 13. Like Figure S 9 but for cluster 3.**

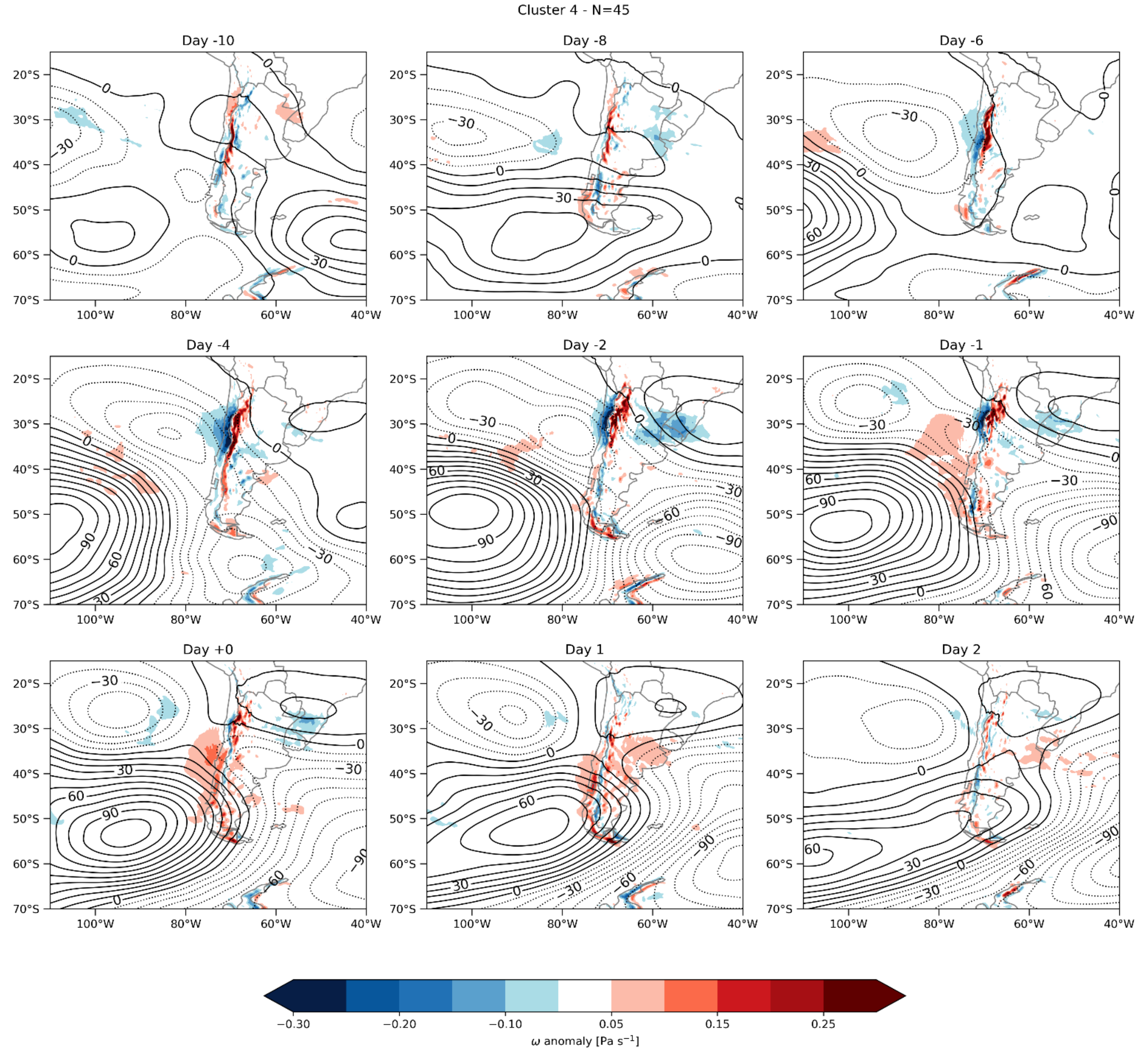


**Figure S 14. Like Figure S 8 but for cluster 4**

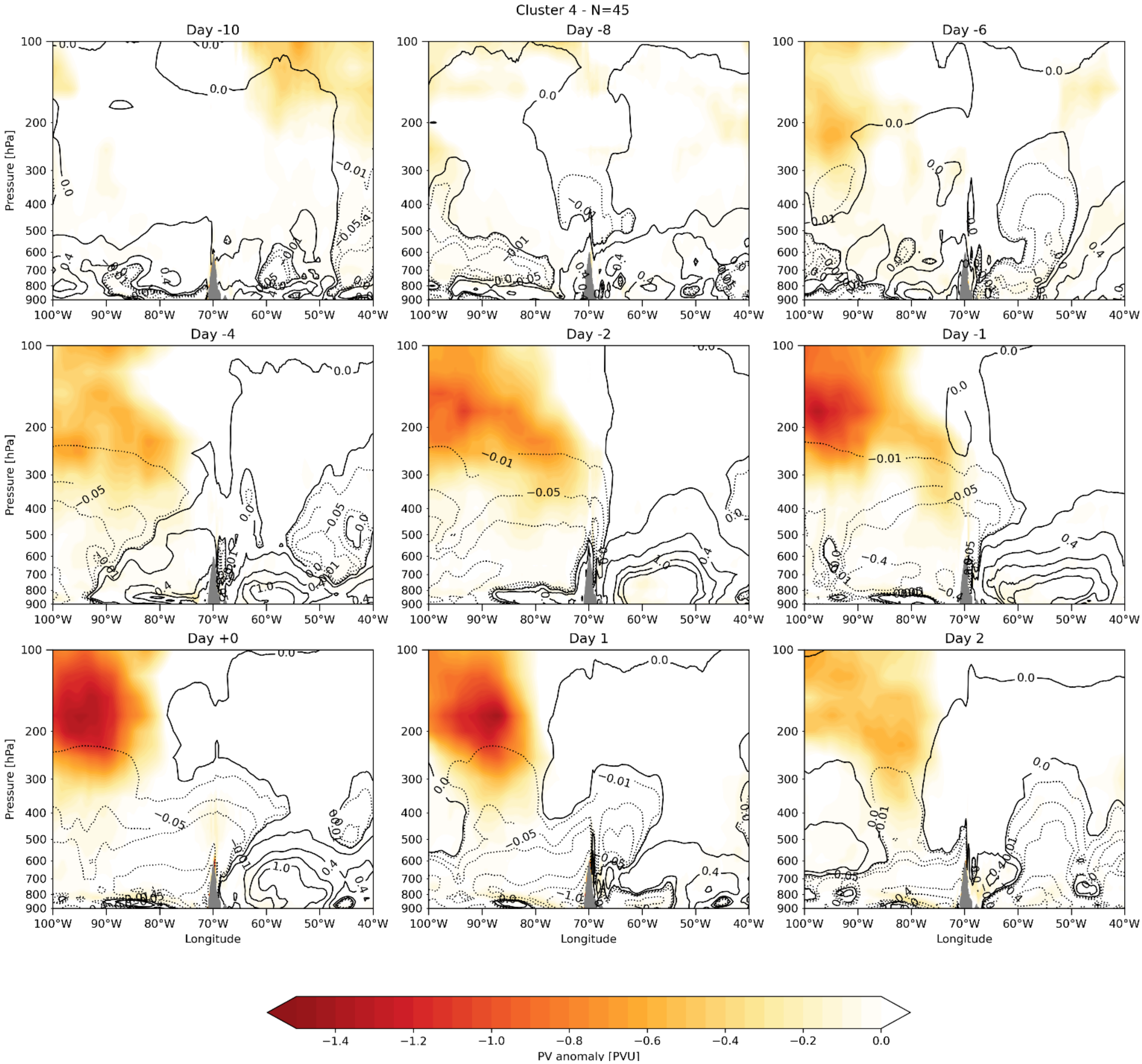


**Figure S 15. Like Figure S 9 but for cluster 4.**

**Back trajectories for representative group members**

We calculated five-day kinematic back-trajectories arriving at Cerro Tololo Inter-American Observatory (CTIO, 30.2°S, 70.8°W) at 700 hPa at the time of maximum surface ozone concentration for each SUTO event (See cluster label and UTC time indicated in the title). Trajectories were computed using ERA5 reanalysis winds (u, v, ω) at 3-hourly, 0.25°resolution on 24 pressure levels (100–925 hPa) with a 4th-order Runge–Kutta scheme (Δt = −1 h). An ensemble of 27trajectories per event is shown, launched from a 3×3 horizontal grid (±0.5° in latitude and longitude) at three pressure levels (650, 700, 750 hPa). Further details are provided in the Figure captions.

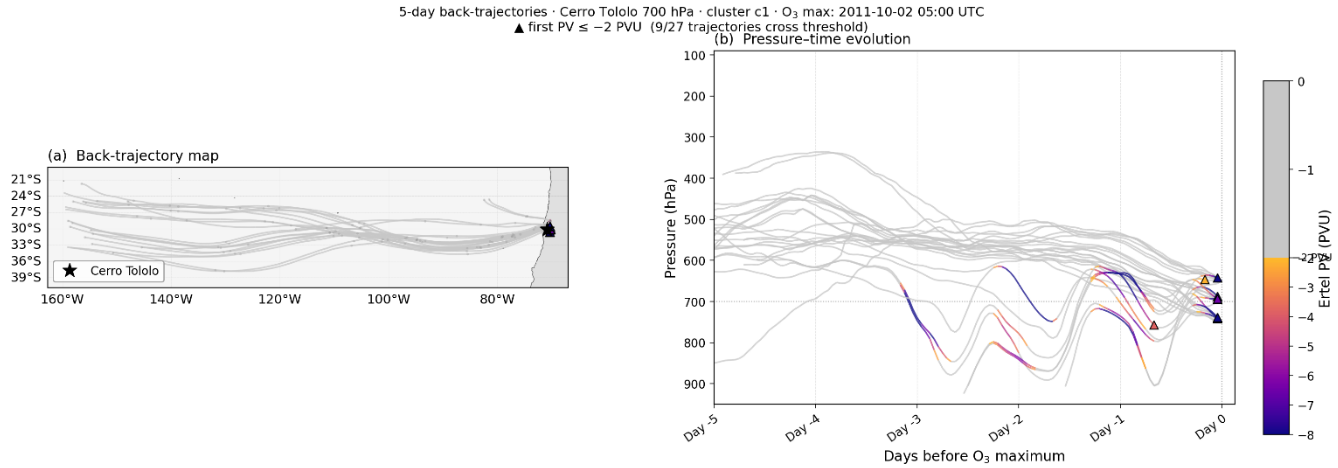


**Figure S 16. (a) Horizontal map of trajectory paths. (b) Evolution of pressure along each trajectory as a function of time before the ozone maximum. In both panels, trajectory segments are colored by Ertel potential vorticity (PV) interpolated along the trajectory path. Segments with PV > −2 PVU are shown in grey(tropospheric air); segments with PV ≤ −2 PVU are colored following the plasma scale (dark purple: most negative PV; yellow orange: near the dynamical tropopause), highlighting air of stratospheric origin. Triangles (▲) mark the first point along each back-trajectory at which PV ≤ −2 PVU is encountered. The number of trajectories that cross this threshold is given in the figure title. The black star denotes the CTIO launch location.**

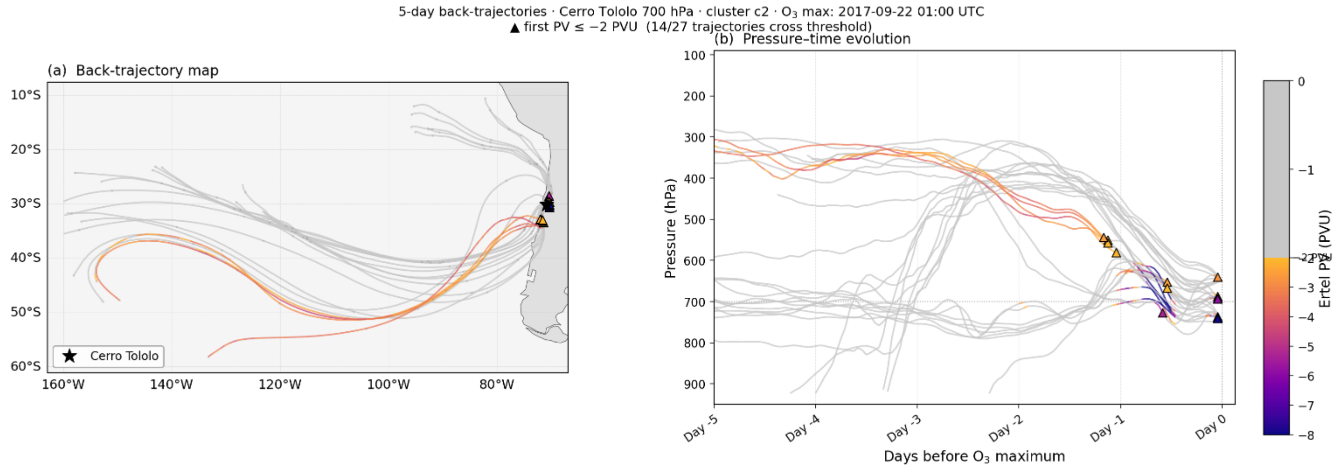


**Figure S 17. As Figure S 16 but for cluster 2.**

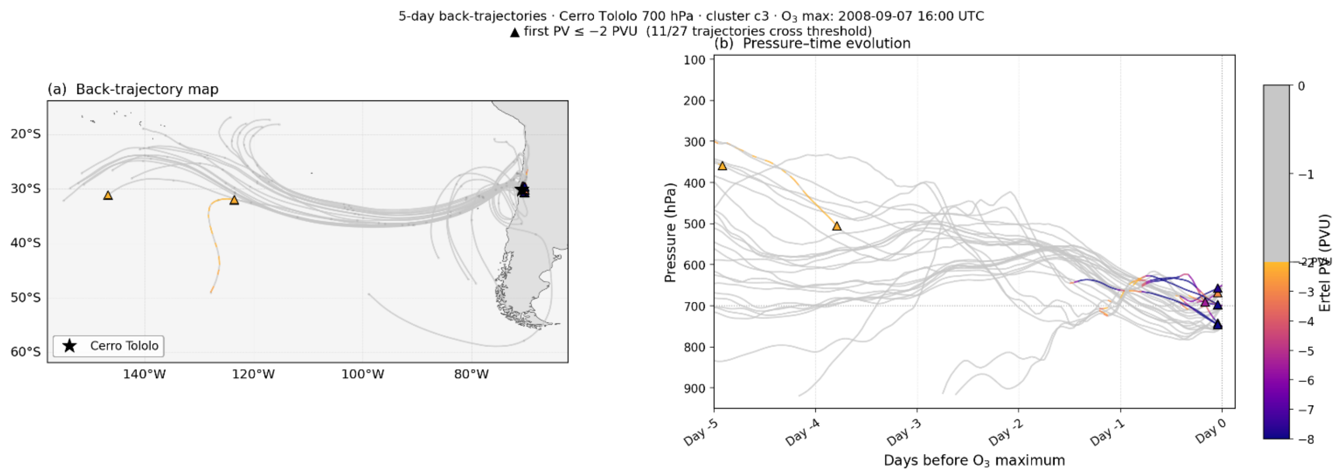


**Figure S 18. As Figure 16 but for cluster 3.**

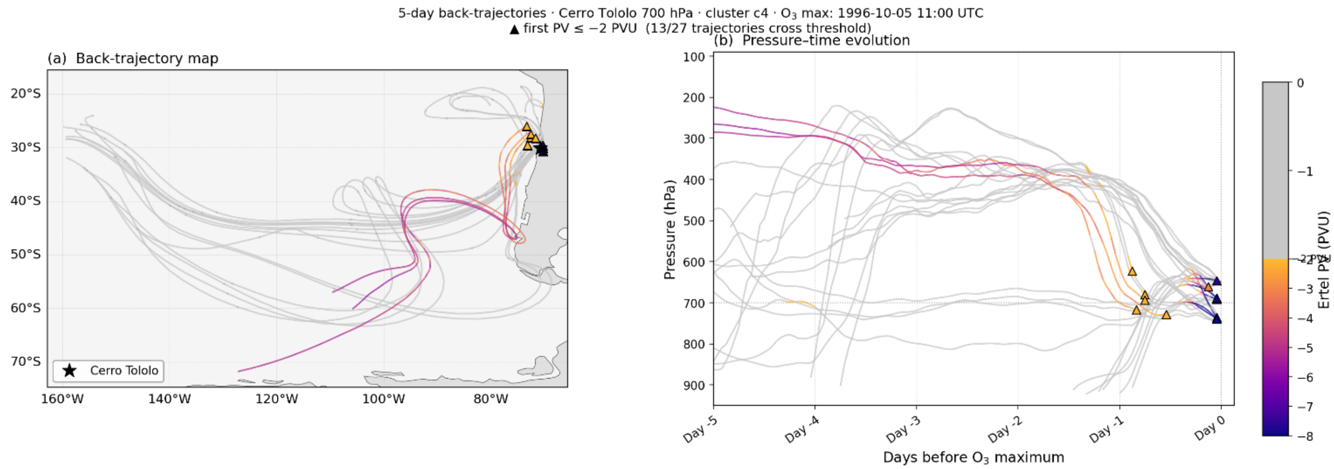


**Figure S 19. As Figure S 16 but for cluster 4.**

1 **SHAP results**

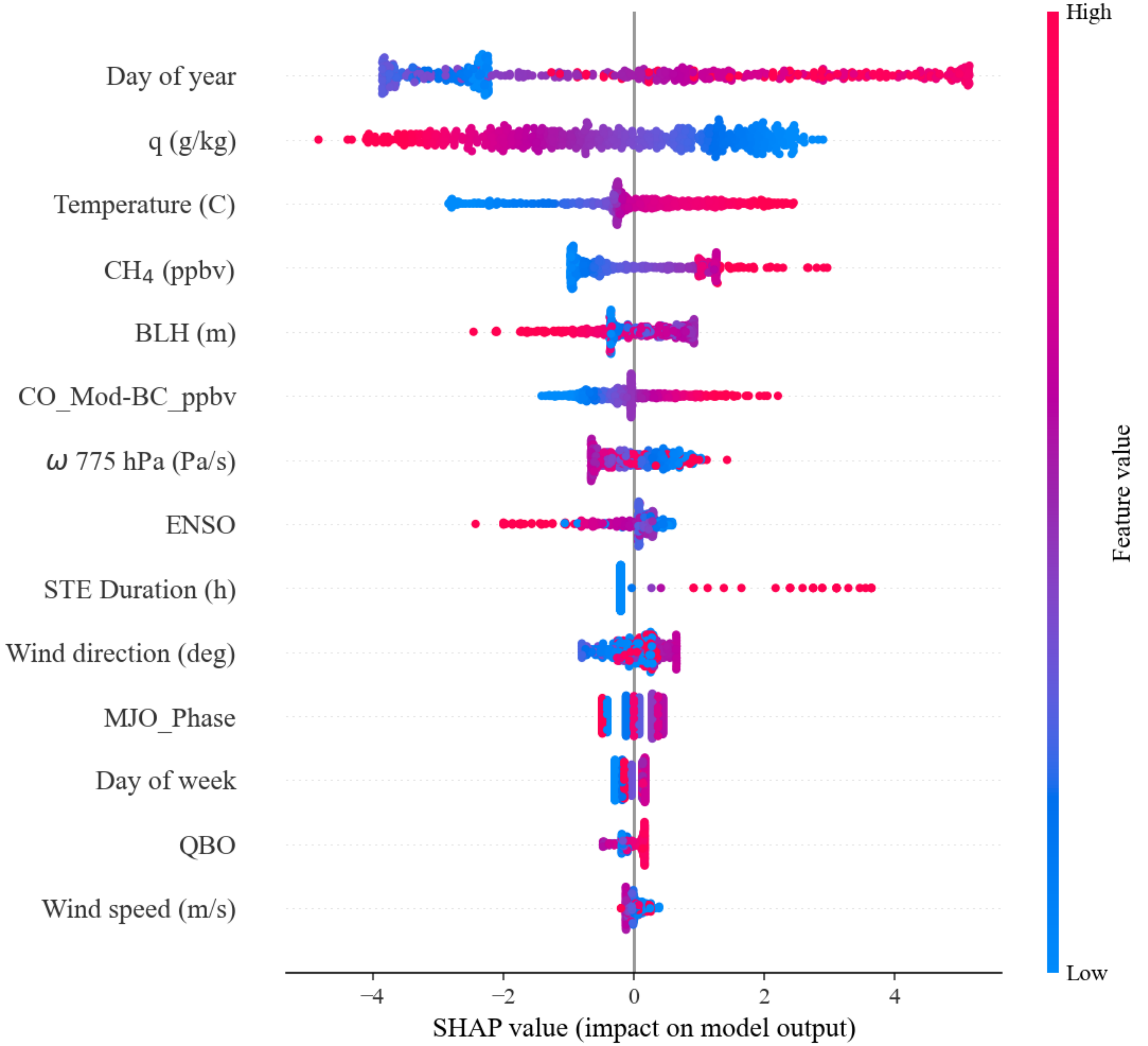


**Figure S 20. Results from the SHAP methodology estimating the relative importance of explanatory variables to ozone at Tololo.**